

## Increasing the Accuracy of Solution NMR Structures of Membrane Proteins by Application of Residual Dipolar Couplings. High-Resolution Structure of Outer Membrane Protein A

Tomasz Cierpicki,<sup>†</sup> Binyong Liang,<sup>†</sup> Lukas K. Tamm,<sup>†</sup> and John H. Bushweller<sup>\*,†,‡</sup>

Contribution from the Department of Molecular Physiology and Biological Physics, University of Virginia, Charlottesville, Virginia 22908, and Department of Chemistry, University of Virginia, Charlottesville, Virginia 22906

Received February 3, 2006; E-mail: jhb4v@virginia.edu

**Abstract:** The structure determination of membrane proteins is one of the most challenging applications of solution NMR spectroscopy. The paucity of distance information available from the highly deuterated proteins employed requires new approaches in structure determination. Here we demonstrate that significant improvement in the structure accuracy of the membrane protein OmpA can be achieved by refinement with residual dipolar couplings (RDCs). The application of charged polyacrylamide gels allowed us to obtain two alignments and accurately measure numerous heteronuclear dipolar couplings. Furthermore, we have demonstrated that using a large set of RDCs in the refinement can yield a structure with 1 Å rms deviation to the backbone of the high-resolution crystal structure. Our simulations with various data sets indicate that dipolar couplings will be critical for obtaining accurate structures of membrane proteins.

### Introduction

Structure determination of integral membrane proteins is becoming one of the most exciting applications of solution NMR spectroscopy. Recent methodological developments are gradually overcoming significant challenges associated with the study of this important class of proteins, and the number of successful structure determinations is growing. NMR can now be routinely used to characterize small  $\alpha$ -helical proteins consisting of one<sup>1,2</sup> or two  $\alpha$ -helices.<sup>3,4</sup> Application of TROSY-based experiments with uniformly deuterated proteins has extended the size limit for studies of membrane protein–detergent complexes beyond 100 kDa and made possible the resonance assignment of several large helical integral membrane proteins.<sup>5,6</sup> Current NMR methodology has been used to define the backbone folds of several moderately sized integral membrane proteins.<sup>7–10</sup>

The paucity of distance information available from the highly deuterated proteins used for these studies calls for new strategies for structure determination. One attractive approach to obtain critical long-range distance information is the application of paramagnetic relaxation enhancement (PRE).<sup>11,12</sup> This approach requires the presence of paramagnetic centers that can be introduced by several methods such as engineering of metal binding sites<sup>13</sup> and site-directed spin-labeling.<sup>11,14</sup> This has been very successfully applied for refinement of the OmpA structure<sup>15</sup> and in the case of the recent structure determination of the putative membrane protein Mistic.<sup>12</sup>

Another very powerful approach for structure determination of membrane proteins involves application of residual dipolar couplings (RDCs). RDCs contain information about the orientation of internuclear vectors relative to the external magnetic field<sup>16,17</sup> and can be readily introduced into structure calculations.<sup>18,19</sup> Measurement of RDCs requires introduction of a weak alignment of the protein molecules in solution. One of the most

<sup>†</sup> Department of Molecular Physiology and Biological Physics.

<sup>‡</sup> Department of Chemistry.

- (1) Park, S. H.; Mrse, A. A.; Nevzorov, A. A.; Mesleh, M. F.; Oblatt-Montal, M.; Montal, M.; Opella, S. J. *J. Mol. Biol.* **2003**, *333*, 409–424.
- (2) Lee, S.; Mesleh, M. F.; Opella, S. J. *J. Biomol. NMR* **2003**, *26*, 327–334.
- (3) Girvin, M. E.; Rastogi, V. K.; Abildgaard, F.; Markley, J. L.; Fillingame, R. H. *Biochemistry* **1998**, *37*, 8817–8824.
- (4) Howell, S. C.; Mesleh, M. F.; Opella, S. J. *Biochemistry* **2005**, *44*, 5196–5206.
- (5) Oxenoid, K.; Kim, H. J.; Jacob, J.; Sönnichsen, F. D.; Sanders, C. R. *J. Am. Chem. Soc.* **2004**, *126*, 5048–5049.
- (6) Trbovic, N.; Klammt, C.; Koglin, A.; Lohr, F.; Bernhard, F.; Dötsch, V. *J. Am. Chem. Soc.* **2005**, *127*, 13504–13505.
- (7) Arora, A.; Abildgaard, F.; Bushweller, J. H.; Tamm, L. K. *Nat. Struct. Biol.* **2001**, *8*, 334–338.
- (8) Fernández, C.; Adeishvili, K.; Wüthrich, K. *Proc. Natl. Acad. Sci. U.S.A.* **2001**, *98*, 2358–2363.
- (9) Hwang, P. M.; Choy, W. Y.; Lo, E. I.; Chen, L.; Forman-Kay, J. D.; Raetz, C. R.; Prive, G. G.; Bishop, R. E.; Kay, L. E. *Proc. Natl. Acad. Sci. U.S.A.* **2002**, *99*, 13560–13565.
- (10) Oxenoid, K.; Chou, J. J. *Proc. Natl. Acad. Sci. U.S.A.* **2005**, *102*, 10870–10875.

- (11) Battiste, J. L.; Wagner, G. *Biochemistry* **2000**, *39*, 5355–5365.
- (12) Roosild, T. P.; Greenwald, J.; Vega, M.; Castronovo, S.; Riek, R.; Choe, S. *Science* **2005**, *307*, 1317–1321.
- (13) Ma, C.; Opella, S. J. *J. Magn. Reson.* **2000**, *146*, 381–384.
- (14) Gaponenko, V.; Howarth, J. W.; Columbus, L.; Gasmí-Seabrook, G.; Yuan, J.; Hubbell, W. L.; Rosevear, P. R. *Protein Sci.* **2000**, *9*, 302–309.
- (15) Liang, B.; Bushweller, J. H.; Tamm, L. K. *J. Am. Chem. Soc.* **2006**, *128*, 4389–4397.
- (16) Prestegard, J. H.; Al-Hashimi, J. H.; Tolman, J. R. *Q. Rev. Biophys.* **2000**, *33*, 371–424.
- (17) Bax, A.; Kontaxis, G.; Tjandra, N. *Methods Enzymol.* **2001**, *339*, 127–174.
- (18) Brünger, A. T.; Adams, P. D.; Clore, G. M.; DeLano, W. L.; Gros, P.; Grosse-Kunstleve, R. W.; Jiang, J. S.; Kuszewski, J.; Nilges, M.; Pannu, N. S.; Read, R. J.; Rice, L. M.; Simonson, T.; Warren, G. L. *Acta Crystallogr., Sect. D: Biol. Crystallogr.* **1998**, *54*, 905–921.
- (19) Schwieters, C. D.; Kuszewski, J. J.; Tjandra, N.; Marius Clore, G. *J. Magn. Reson.* **2003**, *160*, 65–73.

successful media suitable for alignment of protein–detergent complexes is strained polyacrylamide gels.<sup>20–22</sup> Unlike globular proteins, accurate measurement of RDCs for integral membrane proteins is quite difficult,<sup>5,9</sup> and so far only a few examples have been reported. To date, structure refinement using RDCs has been demonstrated for the single transmembrane  $\alpha$ -helical proteins Vpu<sup>1</sup> and Pfl coat protein,<sup>2</sup> to MerF with two transmembrane helices,<sup>4</sup> and pentameric phospholamban.<sup>10</sup>

One of the first structures of an integral membrane protein determined by solution NMR spectroscopy was the transmembrane domain of OmpA.<sup>7</sup> Because of challenges in collecting a significant number of structural restraints, we could only determine the global fold of OmpA. Recently, we developed a series of charged copolymer gels suitable for achieving weak alignment of soluble and integral membrane proteins.<sup>22–24</sup> Application of these gels allowed us to accurately measure RDCs for 19 kDa OmpA in DPC micelles, one of the largest membrane protein systems examined so far.<sup>22</sup> We have measured extensive sets of heteronuclear dipolar couplings for OmpA aligned in two types of polyacrylamide gels. Application of RDCs in combination with previously collected structural restraints allowed us to significantly improve the accuracy of the OmpA structure. In addition, we have evaluated the impact of various types of structural restraints on structure accuracy and discuss general strategies toward structure determination of membrane proteins.

## Experimental Section

**NMR Experiments.** Uniformly <sup>2</sup>H,<sup>13</sup>C,<sup>15</sup>N-labeled OmpA was prepared as described previously.<sup>7</sup> Samples containing 1 mM protein solutions in 600 mM DPC, 10 mM potassium phosphate buffer, pH 6.3, and 50 mM NaCl were used for all NMR experiments. NMR spectra were collected on a cold-probe-equipped Varian Inova 600 MHz spectrometer at 50 °C. For measurements of one-bond (<sup>1</sup>J<sub>HN</sub>, <sup>1</sup>J<sub>C $\alpha$</sub> , <sup>1</sup>J<sub>NC</sub>) and two-bond (<sup>2</sup>J<sub>HNC</sub>) couplings a series of TROSY-based HNCO experiments were used.<sup>25</sup> NMR spectra were then processed in NMRPipe<sup>26</sup> and analyzed in Sparky (T. D. Goddard and J. M. Kneller, University of California, San Francisco). Quality factors (*Q*) have been calculated from the formula  $Q = \text{rms}(D^{\text{calc}} - D^{\text{obs}})/\text{rms}(D^{\text{obs}})$ .<sup>27</sup>

**Measurement and Accuracy of Dipolar Couplings.** Residual dipolar couplings were calculated as the difference between anisotropic and isotropic one-bond couplings (*J* + *D*). Anisotropic couplings were measured for OmpA weakly aligned in two types of polyacrylamide copolymer gels: positively charged (50+M) and negatively charged (50–S).<sup>22</sup> On the basis of duplicate experiments, we estimated the experimental uncertainties of <sup>1</sup>D<sub>HN</sub>, <sup>1</sup>D<sub>C $\alpha$</sub> , and <sup>1</sup>D<sub>NC</sub> couplings to be 1.5, 0.9, and 0.35 Hz, respectively. Since <sup>2</sup>D<sub>HNC</sub> were measured with lower accuracy due to broadening of the proton line width, they were not employed in structure calculations.

**Structure Calculations.** Alignment tensor parameters were obtained from fitting of experimental <sup>1</sup>D<sub>HN</sub> values to the crystal structure (PDB

code 1QJP) using the program Pales.<sup>28</sup> These initial values of the magnitudes and rhombicities of alignment tensors were further optimized in CNS by performing a grid search. These values could easily have been calculated from the powder pattern distribution of the dipolar couplings as well. Finally, we obtained *D*<sub>a</sub> = 14.2 Hz, *R* = 0.07, and *D*<sub>a</sub> = –11.0 Hz, *R* = 0.4 for the 50+M and 50–S data sets, respectively.

Calculation of OmpA structures was carried out using CNS.<sup>18</sup> Several different approaches were used depending on the selection of experimental data (see the Results and Discussion). In all cases, the same simulated annealing protocol was used: 15 ps of torsion angle dynamics at 10000 K was followed by a 100 ps first cooling stage using torsion angle dynamics and a 400 ps second stage of Cartesian dynamics. The force constants for dipolar couplings were adjusted to reflect experimental error. Initial values of 0.001 kcal/(mol Hz<sup>2</sup>) were ramped to 0.5, 0.2, 0.2 kcal/(mol Hz<sup>2</sup>) for <sup>1</sup>D<sub>HN</sub>, <sup>1</sup>D<sub>C $\alpha$</sub> , and <sup>1</sup>D<sub>NC</sub> couplings, respectively. Distances and dihedral angles were restrained with a force constant of 75 kcal/(mol Å<sup>2</sup>) and 400 kcal/(mol rad<sup>2</sup>), respectively. At a final stage the structures were minimized with 10 cycles of conjugate gradient minimization. A total of 140 structures were calculated, and the 10 lowest energy conformers were selected for further analysis.

To compare alignments between the 50+M and 50–S media, we calculated the Euler angles ( $\phi$ ,  $\theta$ , and  $\psi$ ) relating the orientation of the molecular frame to the alignment frame. Values of  $\phi$ ,  $\theta$ , and  $\psi$  obtained for the final set of OmpA structures are  $92.5 \pm 0.2^\circ$ ,  $-12.4 \pm 0.1^\circ$ , and  $-3.4 \pm 6.4^\circ$  for the 50+M data set and  $89.5 \pm 0.2^\circ$ ,  $-22.0 \pm 0.3^\circ$ ,  $76.6 \pm 1.1^\circ$  for the 50–S data set.

## Results and Discussion

**Measurement of Dipolar Couplings.** Measurement of residual dipolar couplings for membrane proteins requires an inert medium that does not interfere with the protein–detergent complex. The recent introduction of polyacrylamide-based gels<sup>20–22</sup> provides just such a medium. Recently, we developed a series of charged polyacrylamide gels that are useful for such measurements. These have been employed to measure dipolar couplings for OmpA in a weakly aligned state.<sup>22</sup> Testing of various gels allowed us to identify positively (50+M) and negatively (50–S) charged copolymers that generate unique alignments for OmpA.

The critical step in achieving high-quality measurement of dipolar couplings was optimization of the degree of sample alignment. Vertical compression of the gel in the NMR tube had to be adjusted to yield the best compromise between the degree of alignment and signal broadening. We found that a degree of alignment yielding maximal <sup>1</sup>D<sub>HN</sub> couplings between 20 and 25 Hz is optimal for accurate measurement of backbone heteronuclear dipolar couplings. For final data collection, we prepared two samples containing [<sup>2</sup>H,<sup>13</sup>C,<sup>15</sup>N]OmpA in DPC micelles soaked in 3.3% 50+M and 4.1% 50–S gels, yielding experimental <sup>1</sup>D<sub>HN</sub> couplings in the range –16 to +25 Hz for 50+M and –20.5 to +15.7 Hz for 50–S.

Four types of heteronuclear dipolar couplings have been measured using TROSY-based HNCO experiments.<sup>25</sup> Three sets of data, <sup>1</sup>D<sub>HN</sub>, <sup>1</sup>D<sub>C $\alpha$</sub> , and <sup>1</sup>D<sub>NC</sub>, could be measured with the high accuracy necessary for structure refinement. In addition, we also obtained <sup>2</sup>D<sub>HNC</sub> couplings albeit with lower accuracy due to signal broadening in the proton dimension. Although these data were not utilized in the structure calculations, we used them for validation. To check whether the two different gel conditions yielded independent alignments, we calculated correlation coefficients between the same types of couplings.

(20) Sass, H. J.; Musco, G.; Stahl, S. J.; Wingfield, P. T.; Grzesiek, S. *J. Biomol. NMR* **2000**, *18*, 303–309.

(21) Chou, J. J.; Gaemers, S.; Howder, B.; Louis, J. M.; Bax, A. *J. Biomol. NMR* **2001**, *21*, 377–382.

(22) Cierpicki, T.; Bushweller, J. H. *J. Am. Chem. Soc.* **2004**, *126*, 16259–16266.

(23) Cierpicki, T.; Bushweller, J. H.; Derewenda, Z. S. *Structure* **2005**, *13*, 319–327.

(24) Lukasik, S. M.; Cierpicki, T.; Borloz, M.; Grembecka, J.; Everett, A.; Bushweller, J. H. *Protein Sci.* **2006**, *15*, 314–323.

(25) Yang, D.; Venters, R. A.; Choy, W. Y.; Kay, L. E. *J. Biomol. NMR* **1999**, *14*, 333–343.

(26) Delaglio, F.; Grzesiek, S.; Vuister, G. W.; Zhu, G.; Pfeifer, J.; Bax, A. *J. Biomol. NMR* **1995**, *6*, 277–293.

(27) Cornilescu, G.; Marquardt, J. L.; Ottiger, M.; Bax, A. *J. Am. Chem. Soc.* **1998**, *120*, 6836–6837.

(28) Zweckstetter, M.; Bax, A. *J. Am. Chem. Soc.* **2000**, *122*, 3791–3792.

**Table 1.** Structural Statistics for the Final OmpA Structure

	no. of restraints	rms dev <sup>a</sup>
distance restraints (Å)	90	0.008 ± 0.001
hydrogen bond restraints <sup>b</sup> (Å)	68	0.009 ± 0.001
dihedral angles <sup>c</sup> (deg)	142	0.067 ± 0.035
RDC (Hz)		
50-S <sup>1</sup> J <sub>HN</sub>	74	1.39 ± 0.019
50-S <sup>1</sup> J <sub>NC'</sub>	72	0.30 ± 0.009
50-S <sup>1</sup> J <sub>C'α</sub>	73	0.83 ± 0.003
50+M <sup>1</sup> J <sub>HN</sub>	71	1.65 ± 0.056
50+M <sup>1</sup> J <sub>NC'</sub>	74	0.37 ± 0.015
50+M <sup>1</sup> J <sub>C'α</sub>	70	0.84 ± 0.001
covalent geometry		
bond lengths (Å)		0.0008 ± 0.00002
bond angles (deg)		0.295 ± 0.004
impropers (deg)		0.166 ± 0.006
structure ensemble <sup>d</sup> (Å)		
backbone		0.48 ± 0.08
heavy atoms		1.86 ± 0.18

<sup>a</sup> Rms deviations for the 10 lowest energy conformers. <sup>b</sup> Two restraints for each hydrogen bond. Hydrogen bonds were only introduced at sites where the pattern of interstrand NH–NH NOEs was consistent with the presence of a hydrogen bond. <sup>c</sup> Number of  $\psi$  and  $\phi$  dihedral angle restraints derived from chemical shifts using TALOS.<sup>30</sup> <sup>d</sup> Rms deviations calculated for residues 5–15, 35–55, 77–100, 122–142, and 162–170.

We obtained an average correlation coefficient of 0.8, indicating these two alignments are not completely unique but do differ significantly.

Previous studies have shown that the  $\beta$ -barrel core of OmpA is relatively rigid while the extracellular loops are highly flexible.<sup>29</sup> For analysis of dipolar couplings, we have selected the well-structured residues 5–15, 35–55, 77–100, 122–142, and 162–170 encompassing most of the  $\beta$ -barrel and including the periplasmic turns. Fitting of RDCs within this fragment to the high-resolution crystal structure of OmpA (PDB code 1QJP) yields good agreement, with  $Q$  factors<sup>27</sup> of 27.2% and 26.1% for 50+M and 50–S alignment media, respectively (see also Table 2).

**Refinement of the OmpA Structure with RDCs.** A low-resolution structure of OmpA has been obtained previously on the basis of application of distance restraints, hydrogen bonds, and chemical-shift-based backbone dihedral angles.<sup>7</sup> To improve the accuracy of the structure, we used an extensive set of dipolar couplings collected from two alignments. We carried out a new set of calculations in CNS using a total of 434 RDCs and previously collected NOE-based distances, hydrogen bonds, and dihedral angles (Table 1). Addition of dipolar couplings in the simulated annealing calculations did not result in violations of the other restraints and resulted in substantial improvement of coordinate precision (Table 1). Since the accuracy of dipolar couplings measured for OmpA is somewhat lower than that typically obtained for globular proteins, we paid particular attention to not overrestrain the RDCs. Thus, force constants have been adjusted to produce rms deviations for dipolar couplings that are consistent with experimental error.

The set of 10 lowest energy structures is shown in Figure 1 and compared to the high-resolution crystal structure. The precision of OmpA coordinates is high, and rms deviations calculated for backbone and heavy atoms within this structured fragment are  $0.48 \pm 0.09$  and  $1.86 \pm 0.18$  Å, respectively. More importantly, we also noticed that application of dipolar couplings significantly improved the backbone accuracy from 1.66 to 1.02 Å (see below).

**Structure of Periplasmic Turns.** The structure of OmpA solved previously using a standard approach without dipolar couplings had a relatively well constrained  $\beta$ -barrel core; however, the periplasmic turns were poorly defined.<sup>7</sup> Measurements of <sup>15</sup>N relaxation times indicate that the residues within the periplasmic  $\beta$ -turns exhibit structural order similar to that of the residues of the barrel itself.<sup>29</sup> This is further supported by the nonaveraged values of the RDCs observed. Therefore, we employed a large number of RDCs measured for residues within the three periplasmic turns. Their use in the refinement resulted in a significant structure improvement, and in most of the calculated conformers we were able to reproduce the conformation of the turns seen in the crystal structure (Figure 2).

The most substantial effect was observed for the second periplasmic turn encompassing residues 86–92. An almost complete set of dipolar couplings has been measured for this fragment. As a consequence, all 10 calculated structures exhibit very similar conformations consistent with the type I turn seen in the crystal structure (Figure 2B). For the two other turns, we also observed significant improvement; however, there are two sets of conformations that are consistent with either type I or type II turns (Figure 2A,C). In the case of the first turn (residues 45–49), 7 out of 10 conformers show the conformation seen in the crystal structure. Similarly, for the third turn (residues 130–136) 6 out of 10 conformers are consistent with the crystal structure. The presence of two conformations results from an insufficient number of dipolar couplings due to the presence of a proline residue in the  $i + 1$  turn position (Pro47 and Pro133). The lack of an amide proton limits the number of observable RDCs and as a consequence the definition of the turn conformation. On the basis of these results we expect that a large number of RDCs can be sufficient to define the conformation of short loops in membrane proteins even in the absence of additional restraints.

**Conformational Heterogeneity.** Detailed analysis of OmpA NMR spectra indicates that in addition to the dominant set of signals numerous amides display additional weaker peaks.<sup>7,31</sup> The origin of this heterogeneity is not known. To probe whether this effect results from local conformational heterogeneity, we measured RDCs for both the major and minor species. Although such measurements have been significantly complicated by weaker intensities and overlap with major peaks, we could determine dipolar couplings for several amides with clearly isolated chemical shifts. Interestingly, for several residues we could clearly identify substantial differences in the magnitude of the anisotropic couplings (Figure 3). Similar results have been obtained for protein aligned in both gels (data not shown). This observation provides direct evidence that the multiplicity of NMR signals results from conformational heterogeneity (Figure 3).

Because of the complexity of the spectra, we could measure dipolar couplings only for the strongest set of peaks. Calculation of  $Q$  factors and further interpretation of dipolar couplings indicates that this predominant conformation of OmpA in DPC micelles is very similar to the conformation seen in the crystal structure. However, a substantial number of residues exist in

(29) Tamm, L. K.; Abildgaard, F.; Arora, A.; Blad, H.; Bushweller, J. H. *FEBS Lett.* **2003**, *555*, 139–143.

(30) Cornilescu, G.; Delaglio, F.; Bax, A. *J. Biomol. NMR* **1999**, *13*, 289–302.

(31) Fernández, C.; Hilty, C.; Bonjour, S.; Adeishvili, K.; Pervushin, K.; Wüthrich, K. *FEBS Lett.* **2001**, *504*, 173–178.



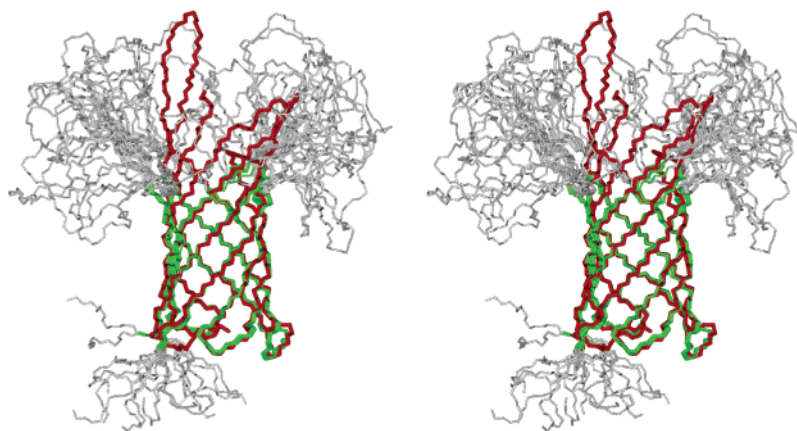


**Figure 1.** Stereofigure showing comparison of the 10 lowest energy conformers of OmpA (green and gray) and the high-resolution crystal structure (red). The structured fragment of OmpA including residues 5–15, 35–55, 77–100, 122–142, and 162–170 is shown in green.

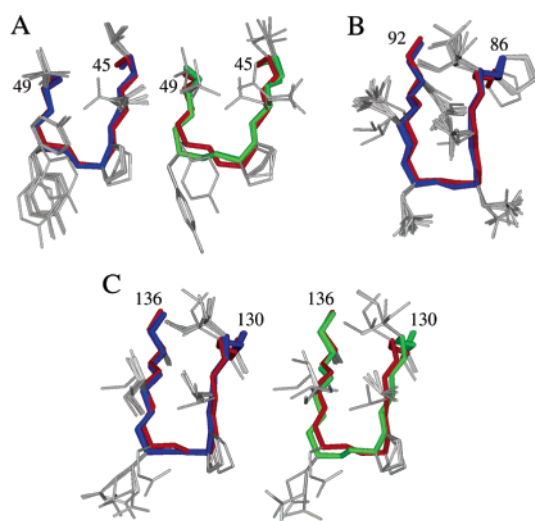


**Figure 2.** Comparison of structures of the three periplasmic turns in the refined structure of OmpA and the high-resolution crystal structure (red). The two conformations observed for turns 1 and 3 (A and C, respectively) are shown in blue and green.

up to two additional conformations that exchange with the major conformation very slowly on the chemical shift time scale. Unfortunately, we were not able to collect a more complete data set for minor species to provide a detailed structural explanation of this effect.

**Impact of Refinement Using Dipolar Couplings.** Dipolar couplings have a significant effect on the accuracy of determined structures;<sup>17,32</sup> however, they must be utilized carefully. It has been demonstrated that the addition of one set of randomly assigned dipolar couplings in the refinement did not cause significant violations of distance restraints and marginally changed the structure.<sup>32</sup> Thus, to monitor whether we indeed observe improvement in the structure accuracy of OmpA, we performed cross-validation with RDCs measured for the second alignment. For this purpose, we also used  $^2D_{\text{HNC}}$  couplings, which, due to lower accuracy, have been omitted from the structure calculations.

First we used RDCs to validate the crystal structure of OmpA. We obtained good agreement, with average  $Q$  factors from different data sets around 28% (Table 2). A higher value of 38–45% was obtained for  $^2D_{\text{HNC}}$ , reflective of the lower

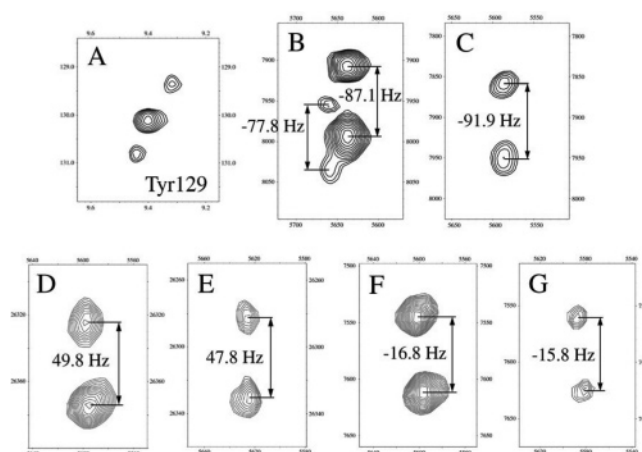


**Figure 3.** Conformational heterogeneity revealed by comparison of anisotropic couplings measured for OmpA in a 50+M gel: (A) spectral region of  $^1\text{H}-^{15}\text{N}$  TROSY-HSQC showing the major and two minor peaks for Tyr129; (B, C) comparison of anisotropic  $^1J_{\text{HN}}$  couplings for three peaks of Tyr129; (D, E) comparison of  $^1J_{\text{C}\alpha}$  couplings for the major (D) and minor (E) peaks for Met53; (F, G) comparison of  $^1J_{\text{NC}}$  couplings for Met53.

**Table 2.** Comparison of  $Q$  Factors<sup>27</sup> (%) for OmpA Calculated Using Different Sets of Restraints

	1QJP <sup>a</sup>	no RDCs <sup>b</sup>	50+M <sup>c</sup>	50-S <sup>d</sup>	50+M and 50-S <sup>e</sup>
50+M $^1D_{\text{HN}}$	27.2	64.7 ± 1.2	14.0 ± 0.32	35.7 ± 0.79	18.1 ± 0.63
50+M $^2D_{\text{HNC}}$	44.9	60.5 ± 3.6	33.0 ± 0.39	36.0 ± 0.07	32.8 ± 0.31
50+M $^1D_{\text{NC}}$	24.7	46.6 ± 0.7	15.7 ± 0.25	25.4 ± 0.17	18.9 ± 0.80
50+M $^1D_{\text{C}\alpha}$	28.1	57.4 ± 2.9	23.8 ± 0.24	31.7 ± 0.75	24.2 ± 0.04
50-S $^1D_{\text{HN}}$	26.1	53.4 ± 3.5	32.7 ± 2.24	11.8 ± 0.71	13.6 ± 0.17
50-S $^2D_{\text{HNC}}$	38.7	66.9 ± 2.4	39.7 ± 1.91	35.1 ± 0.61	34.3 ± 0.18
50-S $^1D_{\text{NC}}$	32.1	58.1 ± 3.4	34.7 ± 3.62	20.8 ± 0.26	23.2 ± 0.79
50-S $^1D_{\text{C}\alpha}$	32.1	64.8 ± 2.1	39.6 ± 0.31	26.5 ± 0.42	29.4 ± 0.11
rms dev <sup>f</sup>		1.66 ± 0.11 <sup>g</sup>	1.11 ± 0.06 <sup>g</sup>	1.16 ± 0.13 <sup>g</sup>	1.02 ± 0.02 <sup>g</sup>
		2.96 ± 0.14 <sup>h</sup>	2.40 ± 0.10 <sup>h</sup>	2.44 ± 0.12 <sup>h</sup>	2.36 ± 0.08 <sup>h</sup>

<sup>a</sup> High-resolution crystal structure (1QJP). <sup>b</sup> Structure calculated without use of dipolar couplings. <sup>c</sup> Structure calculated using the 50+M set of RDCs. <sup>d</sup> Structure calculated using the 50-S set of RDCs. <sup>e</sup> Structure calculated with both sets of RDCs (50+M and 50-S). <sup>f</sup> Rms deviations calculated between the 10 lowest energy conformers calculated using four different strategies (see the text) and the crystal structure for residues 5–15, 35–55, 77–100, 122–142, and 162–170. <sup>g</sup> Rms deviations for backbone atoms. <sup>h</sup> Rms deviations for heavy atoms.

precision of these measurements. This analysis reaffirms that the high-resolution crystal structure of OmpA is consistent with solution data, and as a consequence it can be used to evaluate the accuracy of the NMR structures. On the other hand, the

(32) Bax, A.; Grishaev, A. *Curr. Opin. Struct. Biol.* **2005**, *15*, 563–570.

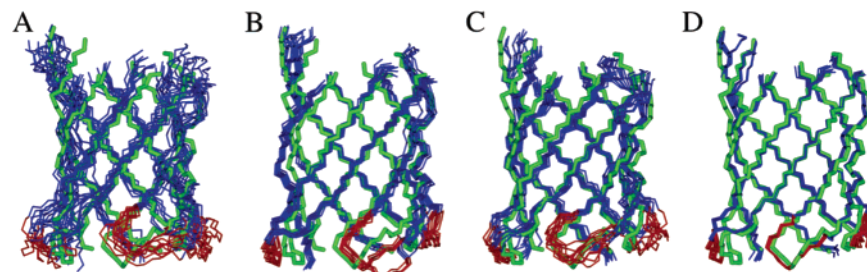


**Figure 4.** Effect of the number of restraints on the precision and accuracy of the OmpA structure. Comparison of the high-resolution crystal structure of OmpA (green) and 10 lowest energy structures calculated with different data sets. The structured part of the protein is shown in blue, and periplasmic turns are in red. Structures have been calculated using (A) distance restraints and dihedral angles, precision  $1.82 \pm 0.22$  Å, accuracy  $2.94 \pm 0.18$  Å, (B) distances, dihedral angles, and RDCs, precision  $0.90 \pm 0.20$  Å, accuracy  $1.92 \pm 0.15$  Å, (C) distance restraints, hydrogen bonds, and dihedral angles, precision  $1.10 \pm 0.15$  Å, accuracy  $1.66 \pm 0.11$  Å, and (D) distance restraints, hydrogen bonds, dihedral angles, and RDCs, precision  $0.48 \pm 0.09$  Å, accuracy  $1.02 \pm 0.02$  Å. Precision is calculated as the backbone rms deviation for backbone atoms among the 10 lowest energy structures, and accuracy is calculated as the rms deviation between the 10 lowest energy structures and the crystal structure.

good agreement between experimental RDCs and the crystal structure reflects the accuracy of the measured dipolar couplings.

To test the impact of dipolar couplings, we carried out four independent calculations. When RDCs were not used in the refinement, we obtained a structure with a  $1.66$  Å backbone rms deviation to the crystal structure. Dipolar couplings poorly correlate with this structure, and  $Q$  factors are around 58% (Table 2). Although the transmembrane barrel is correctly folded, local backbone conformation is weakly restrained due to the very limited number of restraints. In the next step, we carried out two independent calculations separately using RDCs obtained for each of the two alignments. In both cases, we observe a significant drop in the rms deviation to the crystal structure from  $1.66$  to  $1.11$  and  $1.16$  Å for the 50+M and 50-S data sets, respectively. The data set that has not been used in the calculations was employed for the purpose of cross-validation. In both cases we observed substantial improvement, with  $Q$  factors decreased by 10–20% (Table 2). Notably,  $Q$  factors calculated using  $^2D_{\text{HNC}}$  couplings also decreased by 22–27% relative to those of the structure calculated without RDCs.

The final structure calculations combined all data sets with RDCs for two alignments. We observed further improvement of the backbone accuracy to  $1.02$  Å relative to the crystal structure. Final values of  $Q$  factors calculated for the solution structure are somewhat better than those for the crystal structure. A similar trend is observed for the  $^2D_{\text{HNC}}$  couplings that have not been used in the refinement. Although the accuracy of RDCs is not as high as in the case of globular proteins, we demonstrate that this can be overcome by collection of a sufficiently large number of dipolar couplings.

**Strategy for Structure Determination of Membrane Proteins.** Structure determination of moderately sized membrane proteins by NMR spectroscopy currently constitutes a major challenge, and only a handful of structures have been solved so far.<sup>7–10,12</sup> Nevertheless, there are several reports of new targets being investigated.<sup>5,6,33</sup> The transmembrane domain from OmpA is one of the proteins whose structure has been simultaneously determined by NMR spectroscopy<sup>7</sup> and high-resolution X-ray crystallography.<sup>34</sup> Thus, OmpA represents an excellent system to test new approaches for NMR-based structure determination of membrane proteins.

One of the critical issues regarding structure determination of membrane proteins is the limited number of structural restraints which can be collected. To evaluate the impact of various types of restraints, we tested four strategies for structure calculation. In the first approach, we used the data that are most straightforward to obtain in the case of  $\beta$ -barrel proteins, namely, NOE-based backbone–backbone distances and chemical-shift-derived backbone dihedral angles. These data result in a structure with the correct fold, however with poor accuracy and precision (Figure 4A). In the next step, we used additional long-range restraints in the form of interstrand hydrogen bonds, and the accuracy of the structure has been substantially improved from  $2.94$  to  $1.66$  Å (Figure 4C). A comparable improvement was also achieved when, instead of hydrogen bond restraints, we used dipolar couplings in addition to distance and dihedral angle restraints (Figure 4B). We observed an improvement in accuracy from  $2.94$  to  $1.92$  Å, and we also noticed substantial improvement of the backbone precision. The gain in the accuracy was slightly diminished by the fact that two conformations could be distinguished for several residues (Figure 4B). The most substantial improvement was achieved by combination of all data sets (Figure 4D). Using all the data, we were able to obtain a very accurate and precise structure with backbone rms deviation to the high-resolution crystal structure of  $1.02$  Å.

In summary, we emphasize the critical role of dipolar couplings in refinement of structures with sparse restraint data such as integral membrane proteins. For the structured fragment of OmpA, we collected on average 1.4 distances (including hydrogen bonds) and 1.6 backbone dihedral angles per residue. Although these restraints are sufficient to generate the correct fold, only the inclusion of RDCs yielded a structure with a distinct conformation for the periplasmic turns and a substantially improved  $\beta$ -barrel. On the basis of our experience, we expect that similar results can be achieved for  $\alpha$ -helical proteins, provided that an accurate set of RDCs can be measured. In general, application of RDCs will be critical to achieve structures of membrane proteins within  $1$  Å accuracy.

Coordinates for the 10 lowest energy structures of OmpA have been deposited in the Protein Data Bank with accession code 2GE4.

**Acknowledgment.** This work was supported by grants from the National Institutes of Health (R21 GM070825 to J.H.B. and R01 GM051329 to L.K.T.).

(33) Krueger-Koplin, R. D.; Sorgen, P. L.; Krueger-Koplin, S. T.; Rivera-Torres, I. O.; Cahill, S. M.; Hicks, D. B.; Grinius, L.; Krulwich, T. A.; Girvin, M. E. *J. Biomol. NMR* **2004**, *28*, 43–57.

(34) Pautsch, A.; Schulz, G. E. *J. Mol. Biol.* **2000**, *298*, 273–282.